Negative-frequency dispersive wave generation in quadratic media

Matteo Conforti,[1] Niclas Westerberg,[2] Fabio Baronio,[1] Stefano Trillo,[3] and Daniele Faccio[2]
[1]*CNISM, Dipartimento di Ingegneria dell'Informazione, Università di Brescia, Via Branze 38, 25123 Brescia, Italy*
[2]*School of Engineering and Physical Sciences, SUPA, Heriot-Watt University, Edinburgh EH14 4AS, United Kingdom*
[3]*Dipartimento di Ingegneria, Università di Ferrara, Via Saragat 1, 44122 Ferrara, Italy*
(Received 4 December 2012; published 19 July 2013)

We show that the extremely blueshifted dispersive wave emitted in Kerr media owing to the coupling with the negative-frequency branch [E. Rubino *et al.*, Phys. Rev. Lett. **108**, 253901 (2012)] can be observed in quadratic media via second-harmonic generation. Not only is such a phenomenon thus independent of the specific nonlinear mechanism, but it is shown to occur regardless of the fact that the process is pumped by a pulse which exhibits soliton-like features or vice versa undergoes wave breaking. A simple unified formula gives the frequencies of the emitted dispersive waves in both cases.

DOI: 10.1103/PhysRevA.88.013829 PACS number(s): 42.65.Ky, 42.65.Re, 52.35.Tc

I. INTRODUCTION

Solitons emit resonant radiation (RR), also known as Cherenkov radiation, owing to a universal mechanism of phase matching with linear waves ruled by perturbing higher-order dispersive terms. Well-known examples range from fiber [1–3] to Langmuir plasma [4] or water wave [5] solitons. During the last decade, optical fibers offered the unique opportunity to deepen the physics of RR [6–8], with important applicative fallout in supercontinuum generation [9], where RR is responsible for broadening the spectrum over the blueshifted (normally dispersive) region [10]. More recently, the field was significantly advanced by important results recognizing the role of RR in turbulence transport [11], the observation of RR in different settings encompassing tapered [12] and noble-gas-filled photonic crystal fibers [13,14], slow-light waveguides [15], spatial diffraction in arrays [16], and second-harmonic generation (SHG) [17,18]. Importantly, it was also shown that, in Kerr media, new frequencies can be generated owing to the coupling with the negative-frequency part of the spectrum, a process termed negative-frequency resonant radiation (NRR) [19,20]. With reference to this new phenomenon, the aim of this paper is twofold. The first goal is to assess the universal nature of NRR by showing that it can be predicted to occur also in quadratic media under experimentally viable conditions of SHG. In particular, here we restrict ourselves to explore SHG in the regime of large mismatch where the nonlinear phase shifts arise from cascaded conversion and back conversion (cascading [21]). Note, however, that the peculiar features of NRR (large-frequency detunings, overlap of the negative- and positive-frequency content of wave packets) prevent, as explained below, the use of simple nonlinear Schrödinger (NLS) models [22] employed in the past to describe solitons due to cascading (see also review papers in Refs. [23,24]). Second, we generalize the concept of radiation by showing that in fact one does not necessarily need a soliton-like excitation since both the RR and the NRR can be produced also in the *opposite regime* where nonlinearity and group-velocity dispersion (GVD) enforce (instead of compensating) each other. For positive nonlinear shifts (focusing nonlinearity), which we consider here, this occurs when the pump pulse lies in the region of normal GVD. We show that, in this regime, what triggers the radiative mechanism is the occurrence of wave breaking (shock formation) [25,26], with the resonance mechanism made possible by the well-defined velocity of the shock front. It is worth pointing out that, in the regime of *weak* GVD considered here, the cascading leading-order nonlinearity is sufficient to form shock fronts (generally, on both trailing and leading edges of the pulse) even in the absence of other effective terms [27], while the corrections due to group-velocity mismatch [28] are responsible for asymmetries that make the shock occur preferably along one of the pulse edges. In this sense, we can say that the wave breaking is reminiscent of the mechanism observed in experiments performed in the spatial domain [29–31] featuring dispersive shock waves (DSW), whose prediction dates back to the seminal work by Gurevich and Pitaevskii on dispersive hydrodynamics, extended later to the defocusing NLS equation [32]. We also point out that the emission of RR from a pump pulse in the normal dispersion has been recently reported in a fiber experiment performed close to the zero GVD point [33], although without explicitly recognizing the role of wave breaking. Although here we are mainly concerned with the possibility of predicting the emission of NRR in quadratic media, the results presented below along with that of Ref. [33] certainly call for a detailed analysis of the general radiative mechanisms from DSW, which, however, is beyond the scope of this paper and will be faced in the future.

II. RESONANT RADIATION

Let us first explain the general origin of the NRR from a different perspective compared with the analysis of Refs. [19, 20]. We consider an intense pump at carrier frequency ω_p, characterized by a complex envelope $e(t,z)$, which travels with characteristic group velocity v. When such a pulse travels in a nonlinear medium without experiencing significant dispersive effects, its total electric field, which is by definition a real quantity, can be written as $E_p(z,\tau) = e(\tau)\exp[i\bar{k}(\omega_p)z - i\omega_p\tau] + e^*(\tau)\exp[i\bar{k}(-\omega_p)z + i\omega_p\tau]$, where $\tau = t - z/v$ is the retarded time and $\bar{k}(\omega_p) = k(\omega_p) - \omega_p/v + k_{NL}(\omega_p)$, where $k(\omega_p) - \omega_p/v$ is the linear wave number in the moving frame, k_{NL} is the nonlinear correction (phase shift) due to the nonlinearity, and $\bar{k}(-\omega_p) = -\bar{k}(\omega_p)$ for the field to be real. Also linear waves (radiation) at frequency ω can

 ©2013 American Physical Society

be expressed in terms of positive- and negative-frequency content through the real field $E_r(z,t) = A(z)\exp[ik(\omega)z - i\omega t] + A^*(z)\exp[ik(-\omega)z + i\omega t]$. Here $k(\omega) = \omega n(\omega)/c$ is determined by the full dispersive relationship of the material in terms of the real index $n(\omega) = n(-\omega)$, neglecting losses for simplicity. Upon substitution of $t = \tau + z/v$, we cast the radiation in the form $E_r(z,\tau) = A(z)\exp[iD(\omega)z - i\omega\tau] + A^*(z)\exp[-iD(\omega)z + i\omega\tau]$, where $D(\omega) = k(\omega) - \omega/v$ stands for the wave number in a frame comoving with the pump envelope e. Focusing on the positive-frequency content of the radiation, its amplitude $A(z)$ starts to grow due to resonant transfer of energy from the pump at the phase-matching frequency $\omega = \omega_{RR}$ such that $\bar{k}(\omega_p) = D(\omega_{RR})$, which gives the well-known condition for RR [1,3,8,15,17]. Conversely, what it is usually not recognized is the fact that $A(z)$ can be phase matched also with the negative-frequency content of the pump at a different frequency $\omega = \omega_{NRR}$ such that the condition $-\bar{k}(\omega_p) = D(\omega_{NRR})$ is fulfilled. By summarizing, both the phase-matched frequencies $\omega = \omega_{RR}$, ω_{NRR} can be obtained by solving the following unified set of two equations:

$$D(\omega) = \pm\bar{k}(\omega_p). \tag{1}$$

We point out that, owing to symmetry, Eqs. (1) also have solutions $\omega = -\omega_{RR}, -\omega_{NRR}$, i.e., the image frequencies required by the Hermitian symmetry of the radiation field. Moreover, we arrive at Eq. (1) also when starting from the negative-frequency content of the radiation A^*. We emphasize also that, in the following, we directly employ Eqs. (1) to predict resonant frequencies since they give the most general form of resonance (phase matching) by involving the full dispersion relation of the material. However, when the dispersive features are described in terms of a finite number of n-order dispersion coefficients $k_n = \partial^n k/\partial\omega^n|_{\omega_p}$, Eqs. (1) can also be expressed in an equivalent form by resorting to the usual Taylor expansion of the wave number around the frequency ω_p. In particular, starting from $k(\omega) = \sum_{n\geqslant 0}(k_n/n!)\,\delta\omega^n$ and substituting in Eq. (1), we obtain that the frequency detuning $\delta\omega \equiv \omega - \omega_p$ of the resonant radiation is given by the solutions of the following equations [we set $k_p = k(\omega_p)$]:

$$\text{RR}: \sum_{n\geqslant 2}\frac{k_n}{n!}\,\delta\omega^n - \delta\omega\delta k_1 = k_{NL}, \tag{2}$$

$$\text{NRR}: \sum_{n\geqslant 2}\frac{k_n}{n!}\,\delta\omega^n - \delta\omega\delta k_1 + 2k_p - 2\frac{\omega_p}{v} = -k_{NL}, \tag{3}$$

where $\delta k_1 = v^{-1} - v_g^{-1}$ is the inverse velocity difference, with $v_g \equiv k_1^{-1} = (\partial k/\partial\omega|_{\omega_p})^{-1}$ being the natural group velocity at the pump frequency. In the limit $v = v_g$, Eq. (2) recovers the well-known RR formula [3],

$$\sum_{n\geqslant 2}\frac{k_n}{n!}\,\delta\omega^n = k_{NL}, \tag{4}$$

whereas, in the same limit, Eq. (3) reduces to the following condition:

$$2k_p - 2\frac{\omega_p}{v} + \sum_{n\geqslant 2}\frac{k_n}{n!}\,\delta\omega^n = -k_{NL}. \tag{5}$$

III. QUADRATIC MEDIA

In the following, we address the open question as to whether NRR can be observed in a quadratic medium. Our aim is to show that, in such media, Eqs. (1) accurately predict both the RR and NRR frequencies even if the pump pulse is not strictly invariant (strictly nondispersive), provided one is able to accurately estimate its velocity v. In fact, a deviation from the ideal nondispersive behavior of the pump is even beneficial since the growth of RR and NRR become significant when the pump undergoes a strong spectral broadening, thereby seeding the phase-matched radiation frequencies. When nonlinearity and GVD act to mutually balance each other, this requires us to operate with pulses which exhibit compression, i.e., higher-order solitons. However, we go further by showing that also in the opposite regime, where a pulse experiences strong temporal broadening, RR and NRR generation of comparable magnitude can be emitted. In order to demonstrate this, since the radiation detunings can be extremely large, we employ a description based on the numerical integration of the $\chi^{(2)}$ unidirectional pulse propagation equation (UPPE2) implemented for anisotropic media [34–36]. All the details on the implementation of such a method are discussed in Ref. [35], to which we refer the interested reader. This approach is suitable to describe ultrabroadband propagation, not relying on the separation of spectral envelopes around the carriers [17,24]), whose validity breaks down in the regime considered here. Furthermore, although not unique to this approach, the UPPE2 method allows us to account for the full (all orders) dispersion $n(\omega)$ through the Sellmeier equations which characterize any specific material [37].

As a first example we consider a medium with anomalous GVD ($k'' < 0$), with SHG occurring in the regime of high negative mismatch $\Delta k = k(2\omega) - 2k(\omega) < 0$, which results in an effective focusing Kerr nonlinearity, supporting solitary wave propagation [24]. These conditions can be realized, e.g., in a β-BaB_2O_4 (BBO) crystal at carrier wavelength $\lambda_0 = 2\pi c/\omega_0 = 2400$ nm. By exploiting type I ($o + o \to e$) SHG in a crystal with orientation angles $\theta = 45^\circ$ and $\phi = 90^\circ$ (quadratic nonlinear coefficients $|d_{22}| = 2.2$ pm/V and $|d_{31}| = 0.16$ pm/V [37]), we obtain from the Sellmeier equations a phase mismatch $\Delta k = k_e(2\omega) - 2k_o(\omega) = -2.1\times 10^5 m^{-1}$ and a GVD $k'' = -0.18$ ps^2/m. We consider the propagation of an ordinarily polarized hyperbolic secant pulse $\text{sech}(t/t_0)$ with $t_0 = 20$ fs duration. We show typical results obtained for a soliton number $N = \sqrt{L_d/L_{nl}} \simeq 2$, where $L_d = (t_0)^2/|k''|$ and $L_{nl} = [\omega_0 n_{2I} I/c]^{-1}$ (input peak intensity 7.4 TW/cm^2 in vacuum). Here $n_{2I} = -\frac{4\pi}{\lambda_0}\frac{\eta_0}{n^2(\omega_0)n(2\omega_0)}\frac{d_{eff}^2}{\Delta k}$ is the effective Kerr nonlinear index due to cascading, with η_0 being the vacuum impedance. Figure 1 shows the time-domain evolution of the ordinarily polarized electric field [38]. Radiation starts to be emitted at the activation length $z = 1.8$ mm, where the maximal pulse compression and spectral broadening are achieved [see Fig. 2(b)]. After this stage soliton fission occurs with the two constituent solitons separating asymptotically. The temporal evolution in log scale reported in Fig. 1(b) clearly shows that the emitted radiation, which is slower, possesses two distinct branches traveling at different velocities, which turn out to correspond to the RR and the NRR dispersive waves. Indeed the central frequency of these two branches, found

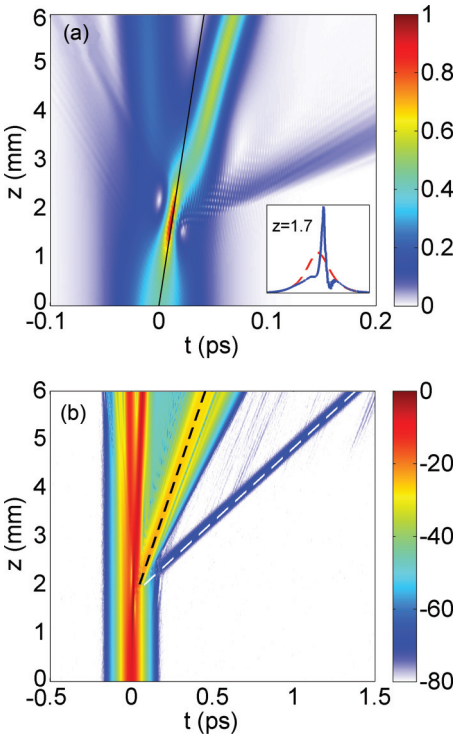

FIG. 1. (Color online) Time-domain electric field [38] evolution in a BBO crystal (ordinary polarization). (a) Linear scale. The black line is the trajectory of a pulse propagating with group velocity $v_g = 0.99876 v_g(\omega_0)$. The inset shows a snapshot at the point maximal compression compared with the input. (b) Same as in (a) but in log scale (dB). Here the dashed black and dashed white lines follow the peaks of the RR ($\lambda = 405$ nm) and the NRR ($\lambda = 575$ nm), respectively.

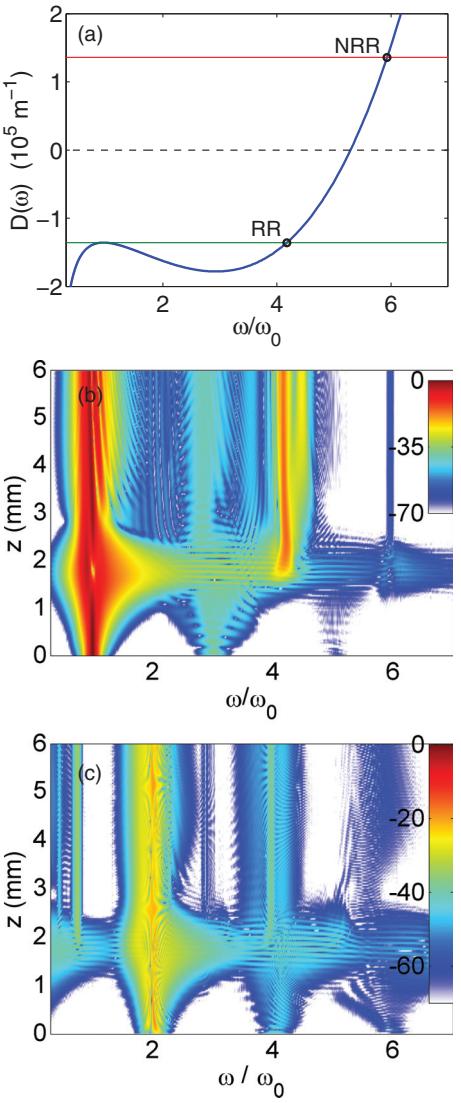

FIG. 2. (Color online) (a) Graphical solution of Eq. (1): the intersections between the blue curve $D(\omega)$ and the red and green horizontal lines, standing for $-\bar{k}(\omega_p)$ and $\bar{k}(\omega_p)$, respectively, give the radiation frequencies $\omega_{RR} = 4.2\,\omega_0$ ($\lambda_{RR} = 575$ nm) and $\omega_{NRR} = 5.95\,\omega_0$ ($\lambda_{NRR} = 405$ nm). Here $\omega_p \equiv 2\pi c/\lambda_0$ ($\lambda_0 = 2400$ nm), $v = 0.99876 v_g(\omega_0)$ (as derived from Fig. 1), and $k_{NL} = 0$ (negligible nonlinear shift). Color level plots of the evolution of the electric field spectrum in log scale: (b) ordinary polarization and (c) extraordinary polarization.

from the spectral evolution in Fig. 2(b) to be $\omega_{RR} = 4.2\,\omega_0$ ($\lambda_{RR} = 575$ nm) and $\omega_{NRR} = 5.95\,\omega_0$ ($\lambda_{NRR} = 405$ nm), is accurately described by Eq. (1). The graphical solution of this equation displayed in Fig. 2(a) shows indeed that such values of ω_{RR} and ω_{NRR} are obtained as the intersection of the dispersion curve $D(\omega)$ with the wave number of the positive- $[\bar{k}(\omega_0)]$ and negative-frequency $[\bar{k}(-\omega_0)]$ components of the pump pulse, respectively. We emphasize that, while the nonlinear phase shift k_{NL} turns out to negligible in this case, it is of paramount importance to accurately estimate the pump velocity v around the activation length where the radiation is emitted since the curve $D(\omega)$ is dramatically affected by even small errors in the value of v. Here we extract the correct value of v from the time-domain evolution, finding $v = 0.99876 v_g(\omega_0)$, which correctly describes the pulse velocity at its maximal compression, as shown by the black line in Fig. 1(a). For the sake of completeness, we also report in Fig. 2(c) the spectral content of the extraordinary wave, which shows the main spectral component at the second harmonic and a weak component at the fourth harmonic.

In the second case we consider the opposite sign of dispersion, namely, normal GVD, but with the same sign of mismatch. Under these conditions, the cascading nonlinearity does not compensate for GVD-induced temporal broadening, but rather enforces it. We have carefully chosen the operating conditions to work in a regime where the nonlinearity initially dominates over the dispersion (i.e., weakly dispersing regime), which is characteristic of the formation of DSW [25,27,29,30]. In this regime, we find viable conditions for the observation of NRR, e.g., in gallium selenide (GaSe), which is characterized by a large nonlinear coefficient $d_{22} = 54$ pm/V [37]. By operating at the central wavelength $\lambda_0 = 2400$ nm with type I ($o + o \rightarrow e$) SHG in a crystal oriented at angles $\theta = 32^\circ$ and $\phi = 90^\circ$, we find from the Sellmeier formulas a phase mismatch $\Delta k = -3.5 \times 10^5$ m^{-1} and a GVD $k'' = 0.32$ ps^2/m. We show in Figs. 3 and 4 the outcome of our simulations obtained from an ordinarily polarized input pulse with 50-fs duration Full Width at Half Maximum Intensity, Gaussian shape, and input peak intensity 500 GW/cm^2

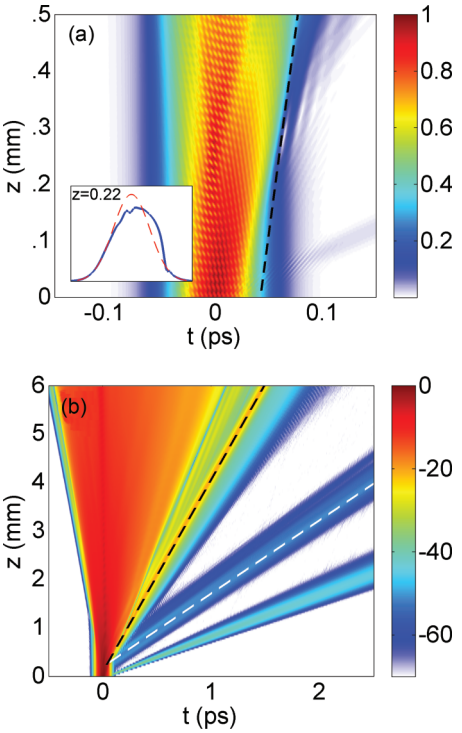

FIG. 3. (Color online) Color level plot of time-domain evolution of the electric field [38] (ordinary polarization): (a) linear scale, early stage ($z \leqslant 0.5$ mm). The inset shows a snapshot at the point of shock formation compared with the input. The black line stands for the shock velocity $v = 0.993 v_g(\omega_0)$. (b) Log (dB) scale, long-range evolution ($z \leqslant 6$ mm). The dashed black and dashed white lines correspond to the RR and the NRR, respectively.

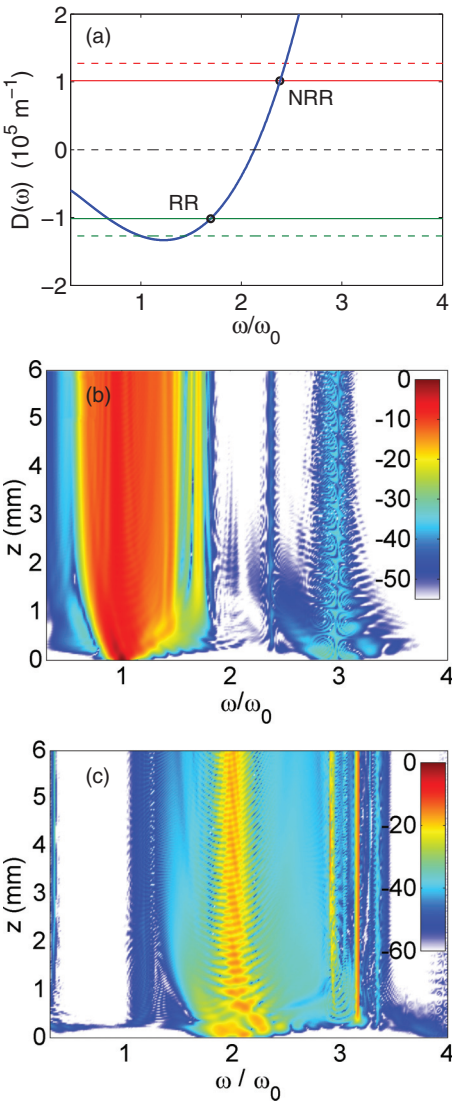

FIG. 4. (Color online) As in Fig. 2 for the case of wave breaking in GaSe described in Fig. 3. In (a) the graphical solutions yielding $\omega_{RR} = 1.7\,\omega_0$ ($\lambda_{RR} = 1410$ nm) and $\omega_{NRR} = 2.37\,\omega_0$ ($\lambda_{NRR} = 1010$ nm) are obtained with the full expression of $\pm\bar{k}(\omega_p)$ (solid horizontal lines), while for comparison the dashed lines stand for the corresponding quantities calculated with $k_{NL} = 0$.

(in vacuum). In this case L_d is several orders of magnitude larger than L_{nl}, and the dynamics is essentially dominated by the nonlinearity. The latter is responsible for the pulse temporal broadening and steepening shown in Fig. 3(a). In particular steepening is found to occur on the trailing edge until a gradient catastrophe leads to the formation of a shock wave (maximal steep front) at $z = z_s \simeq 0.22$ mm [see inset in Fig. 3(a)]. Here the dynamics is essentially different from Kerr media where two symmetric shocks are formed over the leading and trailing edges [25], as also confirmed recently with reference to spatial dynamics [29,30]. The reason is that in SHG the repeated up ($\omega + \omega = 2\omega$) and down conversions ($2\omega - \omega = \omega$) give rise not only to the well-known effective Kerr nonlinearity but also to a leading-order steepening term [28], owing to the group-velocity mismatch, which induces the shock to be asymmetric [27]. Whenever the group velocity at fundamental frequency is sufficiently larger than that at the second harmonic, this term dominates and leads to shock formation on the trailing edge [27,28]. Once formed, the shock front travels with a characteristic velocity which we estimate numerically to be $v = 0.993 v_g(\omega_0)$, while it develops fast oscillations due to the GVD [these occur, in this case, on a small scale due to the absence of a pulse background [27] and hence are not visible in Fig. 3(a)]. The shock formation is accompanied by an abrupt spectral broadening [see Fig. 4(b)] and the consequent emission of radiation. The latter is emitted along two branches, as shown by the temporal evolution in log scale displayed in Fig. 3(b). The different speeds of these branches arise from their different frequencies, which are found from the spectrum in Fig. 4(b) to be $\omega_{RR} = 1.7\,\omega_0$ ($\lambda_{RR} = 1410$ nm) and $\omega_{NRR} = 3.7\,\omega_0$ ($\lambda_{NRR} = 1010$ nm). Also in this case we denoted such frequencies as RR and NRR since they agree perfectly well with the values obtained by the graphical solution of Eq. (1), illustrated in Fig. 4(a). Again, it is crucial to have an accurate estimate of the pump velocity v in the proximity of the radiation emission distance ($z \simeq z_s$). However, in this case the larger nonlinear coefficient d_{eff} results in a non-negligible k_{NL}. Indeed we predict the correct values of ω_{RR} and ω_{NRR} by evaluating k_{NL} as arising from local self-phase modulation, i.e., $k_{NL} = \omega_0 n_{2I} I(z_s,t_s)/c$, with (z_s,t_s) being the location of the shock. We point out that, unlike the previous example, here the two RR and NRR frequencies are redshifted and blueshifted, respectively,

with respect to the second-harmonic frequency. This is also clear from Fig. 4(c), which shows the spectral content of the extraordinary component, where the second harmonic clearly falls in between the two frequencies of the radiation in the ordinary component. In this case the ordinary component in Fig. 4(b) shows also a weak component at $3\omega_0$ that corresponds to the slowest wave in Fig. 3(b), i.e., non-phase-matched third-harmonic generation from the cascaded $o + e \rightarrow o$ process $\omega_0 + 2\omega_0 = 3\omega_0$, whereas the extraordinary component in Fig. 4(c) exhibits also the generation of two frequencies around $3\omega_0$ via nondegenerate phase-matched processes. Importantly, neither of these additional processes, however, hampers the observation of the radiation.

Finally, we point out that $\chi^{(3)}$ nonlinearities can compete with quadratic ones due to the high intensities (especially in the BBO case) involved. However, both BBO and GaSe exhibit a focusing Kerr nonlinear index, which simply results in a lowered intensity threshold for radiation emission without any significant change to the dynamics illustrated above. This is confirmed by additional simulations (not reported) where we account also for the intrinsic Kerr nonlinearity [36].

IV. CONCLUSIONS

In summary, we have demonstrated the generality of the NRR phenomenon by predicting that it can be observed in quadratic media under different scenarios that involve pumping either with soliton-like pulses or in the opposite regime when pulses undergo wave breaking. This represents a substantial step forward toward the understanding and management of ultrafast cascading nonlinearities for producing broadband emission (supercontinuum) in standard crystals.

ACKNOWLEDGMENTS

D.F. acknowledges financial support from the Engineering and Physical Sciences Research Council EPSRC, Grant No. EP/J00443X/1 and from the European Research Council under the European Union's Seventh Framework Programme (FP/2007-2013), ERC Grant Agreement No. 306559. M.C., F.B, and S.T. gratefully acknowledge funding from MIUR (Grant No. PRIN 2009P3K72Z).

[1] P. K. A. Wai, C. R. Menyuk, Y. C. Lee, and H. H. Chen, Opt. Lett. **11**, 464 (1986); **12**, 628 (1987); P. K. A. Wai, H. H. Chen, and Y. C. Lee, Phys. Rev. A **41**, 426 (1990); H. H. Kuehl and C. Y. Zhang, Phys. Fluids B **2**, 889 (1990).

[2] P. Beaud, W. Hodel, B. Zysset, and H. Weber, IEEE J. Quantum Electron. **23**, 1938 (1987); A. S. Gouveia-Neto, M. E. Faldon, and J. R. Taylor, Opt. Lett. **13**, 770 (1988).

[3] N. Akhmediev and M. Karlsson, Phys. Rev. A **51**, 2602 (1995).

[4] V. I. Karpman and H. Schamel, Phys. Plasmas **4**, 120 (1997).

[5] V. I. Karpman, Phys. Rev. E **58**, 5070 (1998).

[6] D. V. Skryabin, F. Luan, J. C. Knight, and P. St. J. Russell, Science **301**, 1705 (2003).

[7] F. Biancalana, D. V. Skryabin, and A. V. Yulin, Phys. Rev. E **70**, 016615 (2004).

[8] D. V. Skryabin and A. V. Gorbach, Rev. Mod. Phys. **82**, 1287 (2010).

[9] J. M. Dudley, G. Genty, and S. Coen, Rev. Mod. Phys. **78**, 1135 (2006).

[10] I. Cristiani, R. Tediosi, L. Tartara, and V. Degiorgio, Opt. Express **12**, 124 (2004).

[11] B. Rumpf, A. C. Newell, and V. E. Zakharov, Phys. Rev. Lett. **103**, 074502 (2009).

[12] S. P. Stark, A. Podlipensky, and P. St. J. Russell, Phys. Rev. Lett. **106**, 083903 (2011).

[13] N. Y. Joly, J. Nold, W. Chang, P. Hölzer, A. Nazarkin, G. K. L. Wong, F. Biancalana, and P. St. J. Russell, Phys. Rev. Lett. **106**, 203901 (2011).

[14] M. F. Saleh, W. Chang, P. Hölzer, A. Nazarkin, J. C. Travers, N. Y. Joly, P. St. J. Russell, and F. Biancalana, Phys. Rev. Lett. **107**, 203902 (2011).

[15] P. Colman, S. Combrié, G. Lehoucq, A. de Rossi, and S. Trillo, Phys. Rev. Lett. **109**, 093901 (2012).

[16] T. X. Tran and F. Biancalana, Phys. Rev. Lett. **110**, 113903 (2013).

[17] M. Bache, O. Bang, B. B. Zhou, J. Moses, and F. W. Wise, Phys. Rev. A **82**, 063806 (2010); C. R. Phillips, C. Langrock, J. S. Pelc, M. M. Fejer, I. Hartl, and M. E. Fermann, Opt. Express **19**, 18754 (2011).

[18] B. B. Zhou, A. Chong, F. W. Wise, and M. Bache, Phys. Rev. Lett. **109**, 043902 (2012).

[19] E. Rubino, J. McLenaghan, S. C. Kehr, F. Belgiorno, D. Townsend, S. Rohr, C. E. Kuklewicz, U. Leonhardt, F. König, and D. Faccio, Phys. Rev. Lett. **108**, 253901 (2012).

[20] E. Rubino, A. Lotti, F. Belgiorno, S. L. Cacciatori, A. Couairon, U. Leonhardt, and D. Faccio, Sci. Rep. **2**, 932 (2012).

[21] R. DeSalvo, D. J. Hagan, M. Sheik-Bahae, G. I. Stegeman, E. W. van Stryland, and H. Vanherzeele, Opt. Lett. **17**, 28 (1992); G. I. Stegeman, M. Sheik-Bahae, E. Van Stryland, and G. Assanto, *ibid.* **18**, 13 (1993); G. I. Stegeman, Quantum Semiclassical Opt. **9**, 139 (1997); C. Conti, S. Trillo, P. Di Trapani, J. Kilius, A. Bramati, S. Minardi, W. Chinaglia, and G. Valiulis, J. Opt. Soc. B **19**, 852 (2002).

[22] A. G. Kalocsai and J. W. Haus, Phys. Rev. A **49**, 574 (1994); R. Schiek, Y. Baek, and G. I. Stegeman, Phys. Rev. E **53**, 1138 (1996).

[23] C. Etrich, F. Lederer, B. A. Malomed, T. Peschel, and U. Peschel, Prog. Opt. **41**, 483 (2000).

[24] A. V. Buryak, P. Di Trapani, D. V. Skryabin, and S. Trillo, Phys. Rep. **370**, 63 (2002).

[25] J. E. Rothenberg and D. Grischkowsky, Phys. Rev. Lett. **62**, 531 (1989).

[26] W. J. Tomlinson, R. H. Stolen, and A. M. Johnson, Opt. Lett. **10**, 467 (1985); D. Anderson, M. Desaix, M. Lisak, and M. L. Quiroiga-Teixeiro, J. Opt. Soc. Am. B **9**, 1358 (1992).

[27] M. Conforti, F. Baronio, and S. Trillo, Opt. Lett. **37**, 1082 (2012); **38**, 1648 (2013).

[28] F. Ö. Ilday, K. Beckwitt, Y.-F. Chen, H. Lim, and F. W. Wise, J. Opt. Soc. Am. B **21**, 376 (2004); J. Moses and F. W. Wise, Phys. Rev. Lett. **97**, 073903 (2006); J. Moses, B. A. Malomed, and F. W. Wise, Phys. Rev. A **76**, 021802(R) (2007).

[29] M. A. Hoefer, M. J. Ablowitz, I. Coddington, E. A. Cornell, P. Engels, and V. Schweikhard, Phys. Rev. A **74**, 023623 (2006).
[30] W. Wan, S. Jia, and J. W. Fleischer, Nat. Phys. **3**, 46 (2007); S. Jia, W. Wan, and J. W. Fleischer, Phys. Rev. Lett. **99**, 223901 (2007).
[31] N. Ghofraniha, C. Conti, G. Ruocco, and S. Trillo, Phys. Rev. Lett. **99**, 043903 (2007); C. Conti, A. Fratalocchi, M. Peccianti, G. Ruocco, and S. Trillo, *ibid*. **102**, 083902 (2009).
[32] A. V. Gurevich and L. P. Pitaevskii, Sov. Phys. JETP **38**, 291 (1974); A. V. Gurevich and A. L. Krylov, *ibid*. **65**, 944 (1987).
[33] K. E. Webb, Y. Q. Xu, M. Erkintalo, and S. G. Murdoch, Opt. Lett. **38**, 151 (2013).
[34] M. Conforti, F. Baronio, and C. De Angelis, Phys. Rev. A **81**, 053841 (2010); IEEE Photonics J. **2**, 600 (2010).
[35] M. Conforti, F. Baronio, and C. De Angelis, J. Opt. Soc. Am. B **28**, 1231 (2011).
[36] M. Conforti and F. Baronio, J. Opt. Soc. Am. B **30**, 1041 (2013).
[37] D. N. Nikogosyan, *Nonlinear Optical Crystals: A Complete Survey* (Springer, Berlin, 2005).
[38] We display the inverse Fourier transform of the positive-frequency components of the spectrum. This allows us to directly visualize the envelope, eliminating the fast oscillations of the carrier while retaining the full broadband features of the spectrum.